

# The Effects of Increasing Seasonal Dynamism when Predicting Connectivity: Advantages or Unnecessary Complications?

David D. Hofmann<sup>1,2,§</sup>  Dominik M. Behr<sup>1,2</sup>  John W. McNutt<sup>2</sup>  
Arpat Ozgul<sup>1, 2</sup>  Gabriele Cozzi<sup>1,2</sup> 

May 8, 2024

<sup>1</sup> Department of Evolutionary Biology and Environmental Studies, University of Zurich,  
Winterthurerstrasse 190, 8057 Zurich, Switzerland.

<sup>2</sup> Botswana Predator Conservation Program, Wild Entrust, Private Bag 13, Maun,  
Botswana.

§ Corresponding author: david.hofmann2@uzh.ch

**Running Title:** Connectivity in Seasonal Landscapes

**Keywords:** African wild dog, Connectivity, Dispersal, Dynamism, Individual-based,  
*Lycaon pictus*, Okavango Delta, Seasonality

## Abstract

Seasonally changing conditions can drastically alter landscape connectivity. Nevertheless, most connectivity studies ignore seasonal dynamism and instead employ a static set of spatial covariates and assume their focal species to exhibit a static set of preferences. Ignoring seasonality may, however, mask important ecological features and processes, thus resulting in poor agreement between predicted and observed movements and a misrepresentation of connectivity.

We present a simple framework highlighting that seasonality may enter a connectivity analysis at three distinct stages, namely when (1) extracting spatial covariates for model fitting, (2) when fitting the selection model, and (3) when making predictions from the fitted model. In combination, this provides six possible configurations that differ in terms of the seasonal dynamism they encapsulate.

Capitalizing on natural seasonal fluctuations of the Okavango Delta in northern Botswana and on GPS data collected on dispersing African wild dogs (*Lycaon pictus*) across different seasons, we investigate the degree to which a better representation of seasonal dynamism improves our ability to predict connectivity. For this, we fit integrated step-selection functions and predict connectivity using an individual-based dispersal simulation while explicitly considering seasonal dynamism in both environmental covariates and the species' preferences. Using a rigorous cross-validation procedure, we compare the predictive model performance under each of the six proposed configurations. While we expected that an increasing degree of seasonal dynamism would lead to improved predictions, we were particularly interested in identifying at which stage the inclusion of seasonality provides the biggest benefits.

We show that, for our study system, improvements in predictive performance by incorporating seasonal dynamism were moderate. In fact, incorporating seasonality only improved predictions when an overly simplistic movement model was assumed. Upon fitting a more complex model, the benefits of accounting for seasonality vanished, resulting in imperceptible performance differences. Despite this, patterns of connectivity as obtained from dispersal simulations revealed marked differences between the most static and most dynamic configurations. Most notably, connectivity was more homogeneously distributed throughout the study area when seasonality was taken into account, suggesting the existence of seasonal stepping stones that facilitate dispersal into otherwise inaccessible areas.

Besides a better understanding of the importance of dynamic connectivity, our results also provide insights into the conservation needs of the endangered African wild dog.

# Contents

<b>1</b>	<b>Introduction</b>	<b>1</b>
1.1	Connectivity . . . . .	1
1.2	Seasonality . . . . .	1
1.3	Modeling Functional Connectivity . . . . .	2
1.4	Incorporating Seasonality in Functional Connectivity Models . . . . .	3
1.5	African wild dogs in Northern Botswana . . . . .	3
1.6	What We Did . . . . .	4
<b>2</b>	<b>Methods</b>	<b>5</b>
2.1	Study Area . . . . .	5
2.2	GPS Data . . . . .	6
2.3	Covariates . . . . .	6
2.3.1	Landscape Characteristics . . . . .	7
2.3.2	Climate Descriptors . . . . .	8
2.3.3	Anthropogenic Features . . . . .	8
2.3.4	Light Availability . . . . .	8
2.4	Step-Selection Models . . . . .	9
2.5	Validation . . . . .	11
2.6	Simulations . . . . .	11
<b>3</b>	<b>Results</b>	<b>12</b>
3.1	Step-Selection Models . . . . .	12
3.2	Validation . . . . .	13
3.3	Simulations . . . . .	13
<b>4</b>	<b>Discussion</b>	<b>14</b>
4.1	Brief Summary . . . . .	14
4.2	Moderate Improvements upon Increasing Dynamism . . . . .	14
4.3	Substantial Improvements upon Fitting a Complex Model . . . . .	15
4.4	Dynamic Connectivity . . . . .	15
4.5	The Costs of Incorporating Dynamism . . . . .	16
4.6	Validation Procedure . . . . .	17
4.7	Seasonal Habitat Selection . . . . .	18
4.8	Conclusion . . . . .	18
<b>5</b>	<b>Authors' Contributions</b>	<b>19</b>
<b>6</b>	<b>Data Availability</b>	<b>19</b>
<b>7</b>	<b>Acknowledgments &amp; Funding</b>	<b>19</b>

# **1 Introduction**

## **2 1.1 Connectivity**

3 Landscape connectivity is defined as the degree to which the landscape facilitates or impedes  
4 movement among habitat patches (Taylor et al., 1993) and is a critical prerequisite for  
5 maintaining biodiversity (Fahrig, 2003). Improved connectivity facilitates dispersal (Doerr  
6 et al., 2011; Baguette et al., 2013), which in turn promotes genetic diversity (Perrin and  
7 Mazalov, 2000; Frankham et al., 2002) and the colonization of vacant habitats (Hanski, 1999;  
8 MacArthur and Wilson, 2001). Due to its beneficial impacts on metapopulation dynamics,  
9 restoring connectivity is among the most frequently recommended strategies to conserve  
10 biodiversity and to promote resilience against climate change (Heller and Zavaleta, 2009;  
11 Rudnick et al., 2012). Quantifying connectivity and identifying critical dispersal corridors  
12 have therefore become critical tasks in conservation science (Heller and Zavaleta, 2009;  
13 Rudnick et al., 2012; Keeley et al., 2019; Hofmann et al., 2021). One aspect that has received  
14 limited attention in the study of connectivity is the role of seasonality. Yet, seasonal changes  
15 both in the environment and in an animal's propensity to use or avoid particular habitat  
16 types can profoundly impact landscape connectivity (Zeller et al., 2020a).

## **17 1.2 Seasonality**

18 Seasonality can impact functional connectivity through spatio-temporal variation in the  
19 landscape itself, or through temporal variation in species' preferences towards prevailing  
20 conditions (Mui et al., 2017; Simpkins and Perry, 2017; Zeller et al., 2020a). In ecosystems  
21 that experience alternations between wet and dry seasons, for example, the onset of the rainy  
22 season initiates distinct "green-up" waves, which affect the availability of food resources for  
23 herbivores and, subsequently, shape their movements (Merkle et al., 2016). In its most re-  
24 markable form, the variation in environmental conditions drives herbivore migrations across  
25 massive spatial scales, resulting in short-lived movement corridors between two otherwise  
26 disconnected habitats (Serneels and Lambin, 2001; Naidoo et al., 2016). Alternatively, sea-  
27 sonality can affect functional connectivity via temporal changes in a species' movement and  
28 habitat preferences. Amphibians, for instance, require both aquatic and terrestrial habitats,  
29 but their preference for one over the other heavily depends on the season (Baldwin et al.,  
30 2006). Although such seasonal intricacies are likely to play a fundamental role in many  
31 ecosystems, they only rarely enter connectivity studies in an explicit manner. In fact, most  
32 connectivity studies represent their study system by a static set of environmental layers and

assume that their focal species exhibits a fixed set of preferences (e.g., Elliot et al., 2014; Abrahms et al., 2017; Brennan et al., 2020). However, this may result in biased connectivity estimates and a misallocation of scarce conservation funds (Osipova et al., 2019; Zeller et al., 2020b). Therefore, a more dynamic approach to connectivity that acknowledges and renders seasonal variation has been recommended (Zeller et al., 2020a).

### 1.3 Modeling Functional Connectivity

Functional connectivity can be estimated using a variety of modeling techniques (Diniz et al., 2019), which all comprise four main steps. First, presence data of the focal species, preferably collected during dispersal (Elliot et al., 2014; Vasudev et al., 2015; Benz et al., 2016, but see Fattebert et al., 2015), and a set of spatial covariate layers that are believed or known to be critical determinants of connectivity are compiled. Second, these data are combined and fed into a selection model that enables estimating a species selection or avoidance of environmental features. Popular frameworks for estimating preferences are case-control designs, where characteristics extracted at observed locations are contrasted with characteristics extracted at available locations (Beyer et al., 2010; Fieberg et al., 2010). This can be achieved using point-selection functions (Boyce et al., 2002; Manly et al., 2007), path-selection functions (Cushman and Lewis, 2010), and step-selection functions (Fortin et al., 2005; Thurfjell et al., 2014). A particularly powerful approach is that of *integrated* step-selection functions (iSSFs), as it provides an effective means to model both an animal's habitat-selection and movement capacity (Avgar et al., 2016; Fieberg et al., 2021). Third, inferred preferences are used to predict a permeability surface, which indicates the expected ease or difficulty at which the focal species can traverse a certain area given the area's environmental characteristics (Zeller et al., 2012). Finally, in a fourth step, the permeability surface serves as an input to a connectivity model that reveals crucial movement corridors. At present, the most popular connectivity models are least-cost path analysis (Adriaensen et al., 2003) and circuit theory (McRae et al., 2008), although individual-based movement models (IBMMs) have gained some momentum recently (Kanagaraj et al., 2013; Allen et al., 2016; Hauenstein et al., 2019; Zeller et al., 2020b; Unnithan Kumar et al., 2022a,b; Hofmann et al., 2023). In particular, some IBMMs allow estimating connectivity directly via simulated dispersal trajectories, thus bypassing the generation of a permeability surface (Unnithan Kumar et al., 2022a; Hofmann et al., 2023).

**64 1.4 Incorporating Seasonality in Functional Connectivity Models**

65 Seasonality can enter the connectivity modeling workflow described above in three distinct  
66 stages (Figure 1). In the first stage, one can either extract environmental features, such as  
67 water and vegetation, from a static layer (i.e., a single snapshot) or from a time series of  
68 layers (i.e., a sequence of snapshots) that capture seasonal variation across the landscape.  
69 The former approach has historically been the norm (e.g., Elliot et al., 2014; Brennan et al.,  
70 2020), yet advances in remote sensing technologies and a facilitated access to petabytes of  
71 landscape data have opened up new avenues for obtaining spatial layers at unprecedented  
72 spatio-temporal resolutions (Toth and Józków, 2016; Rumiano et al., 2020), such that the  
73 representation of study systems via dynamic covariate layers has become more frequent  
74 (e.g., Osipova et al., 2019; Kaszta et al., 2021). In a second stage, one can assume their  
75 focal species to exhibit a fixed set of preferences across seasons by pooling all presence data,  
76 or can try to account for seasonal changes in preferences by splitting the data accordingly  
77 (e.g., Fortin et al., 2005; Manly et al., 2007; Cushman and Lewis, 2010; Zeller et al., 2020b).  
78 Chetkiewicz and Boyce (2009), for instance, partitioned their data by season to derive sea-  
79 sonal habitat preferences for pumas (*Puma concolor*) and grizzlies (*Ursus arctos*). In a final  
80 stage, one can estimate connectivity for either “average” environmental conditions, or utilize  
81 seasonally updated layers to estimate connectivity for distinct seasons. For connectivity  
82 models that rely on permeability surfaces, this implies repeatedly applying the connectivity  
83 model using seasonally updated resistance surfaces (e.g. Osipova et al., 2019; Zeller et al.,  
84 2020b; Kaszta et al., 2021; Ciudad et al., 2021). This is demonstrated *ad extremum* by  
85 Kaszta et al. (2021), who prepared monthly updated permeability surfaces for African ele-  
86 phants (*Loxodonta africana*). The above-mentioned IBMMs allow for an elegant solution,  
87 for seasonality can be accounted for as simulated individuals move. Such an approach has,  
88 however, not yet been followed. Irrespective of the method used, including seasonality is  
89 analytically and computationally demanding (Bishop-Taylor et al., 2018), raising the ques-  
90 tion to what degree it should be considered. Our goal is (1) to create a framework with the  
91 possible combinations in which seasonality can be accounted for, (2) to establish whether  
92 incorporating seasonality benefits the predictive performance of connectivity analyses, and  
93 (3) to pinpoint at which stages the inclusion of seasonality provides the largest benefit.

**94 1.5 African wild dogs in Northern Botswana**

95 A system well-suited to study the importance of seasonal dynamism for dispersal and connec-  
96 tivity is the African wild dog population (*Lycaon pictus*) inhabiting the seasonally highly

variable Okavango Delta ecosystem in northern Botswana (McNutt, 1996; Wolski et al., 2017). While once present across the entire Sub-Saharan continent, the African wild dog has disappeared from a majority of its historic range due to human persecution, deadly diseases, and habitat destruction (Woodroffe et al., 2020). With about 6,000 adult individuals remaining in the wild, the species is considered as endangered on the IUCN red list. Wild dogs are pack-living carnivores, primarily active during the cooler morning and evening hours (Rasmussen and Macdonald, 2012) or during moonlit nights (Cozzi et al., 2012). Higher ambient temperature is associated with shorter activity periods, as the species usually rests during times of elevated heat (Rabaiotti and Woodroffe, 2019). Upon reaching sexual maturity, individuals born into a pack disperse in single-sex coalitions to find suitable mates and a territory to settle (McNutt, 1996). In Botswana, the timing of dispersal is seasonal, with female dispersal peaking prior to the mating season in March, and male dispersal peaking at the onset of the rainy season in December (Behr et al., 2020). Euclidean distances moved by dispersers range from 5 km to 500 km, with some coalitions covering several hundred kilometers within only a few days (Davies-Mostert et al., 2012; Masenga et al., 2016; Cozzi et al., 2020; Sandoval-Seres et al., 2022). Studies of habitat-selection during dispersal show that wild dogs avoid water, prefer moving along it, prefer moving across open grass or shrubs, yet avoid areas dominated by humans and densely covered by forests (O'Neill et al., 2020; Hofmann et al., 2021).

## 1.6 What We Did

Here, we examined the importance of including seasonally-varying factors to assess landscape connectivity for the African wild dog. For this, we compared the predictive performance of iSSFs that differ in terms of the dynamism they represented. Specifically, we investigate if and to what degree seasonality at different stages of the connectivity modeling workflow contributes to improved predictions. For this, we compile an extensive collection of remote sensed time series data that accurately render seasonality across the Okavango Delta ecosystem. We combine them with multi-year dispersal data from 30 dispersing wild dog coalitions in northern Botswana and apply k-fold cross-validation for case-control studies to compare the predictive efficacy of each model. Finally, we employ IBMMs to simulate dispersal and estimate connectivity resulting from varying degrees of dynamism. We hypothesized that habitat-selection and movement behavior would differ significantly between seasons and that increasing the degree of dynamism would result in better agreement between observed and predicted dispersal patterns (Figure 1).

130 **2 Methods**

131 We used the R programming language (R Core Team, 2023) for all data preparation and  
132 analyses. We performed spatial data manipulation using the `terra` (Hijmans et al., 2024)  
133 and `spatstat` (Baddeley et al., 2015) packages. We generated figures using the `ggplot2`  
134 (Wickham et al., 2024) and `ggpubr` (Kassambara, 2024) packages. To ensure reproducibility  
135 of all our analyses, we provide access to our R-scripts through an online repository upon  
136 publication of this article.

137 **2.1 Study Area**

138 The study area comprised the Okavango Delta ecosystem, mainly within northern Botswana  
139 (centered at 24°30'E 20°42'S at an elevation of approx. 950 m) but also extended to parts  
140 of Namibia and Zimbabwe, and stretched across an extent of 160,000 km<sup>2</sup> (Figure 2). The  
141 Okavango Delta is a flood-pulse driven mosaic of patchy woodlands, permanent swamps, and  
142 seasonally flooded grasslands that lie within the otherwise dry and sandy Kalahari Basin  
143 (Wilson and Dincer, 1976; Ramberg et al., 2006; Mendelsohn et al., 2010). Precipitation  
144 across the study area varies considerably between seasons, ranging from 0 mm during the dry  
145 season (from ~ 15 April to 15 October) to 140 mm during the wet season (from ~ 15 October  
146 to 15 April), totaling to 600 mm across an average year (Figure 3a). Daily maximum above-  
147 ground temperature fluctuates between 7°C during the dry winter months to 38°C during  
148 the wet summer months (Figure 3b). The vegetation in the study area is mainly composed  
149 of mopane forest (*Colophospermum mopane*), mixed woodland acacia-dominated (*Acacia*  
150 *spp.*), and grassland. Substantial vegetation green-up (e.g., plant and shoots growth, leaf  
151 production, grass greening) after the dry season starts with a delay of some weeks after  
152 the onset of the first rains in the wet season. The normalized difference vegetation index  
153 (NDVI) therefore depicts a lagged response to precipitation patterns across the study area  
154 (Figure 3c). The yearly flood-cycle of the Delta is predominantly driven by rainfalls in the  
155 Angolan highlands, where water is collected and channeled through the Cubango and Cuito  
156 rivers into the Okavango Delta (McCarthy et al., 2003; Gumbrecht et al., 2004; Mendelsohn  
157 et al., 2010). Because water only slowly descends from the catchment areas in Angola  
158 into the Delta's tributaries, the flood is out of sync with local rainfalls and reaches its  
159 maximum extent during August-September, i.e. during peak dry season (Wolski et al.,  
160 2017, Figure 3d). While the extent of large-bodied rivers and floodplains is determined by  
161 precipitation in Angola, the emergence of smaller, ephemeral water-bodies (a.k.a., pans) is  
162 dictated by local precipitation during the wet season. 62% of the landscape in the study area

163 form part of a protected area, such that human impact remains low and largely limited to  
164 settlements along the western part of the delta and the city of Maun at the delta's southern  
165 tip (Figure 2). Landscapes outside protected areas in Zimbabwe, however, are more heavily  
166 influenced by humans, mainly through agricultural fields and human settlements.

## 167 2.2 GPS Data

168 Between 2015 and 2022, we collected GPS data of 30 dispersing wild dog coalitions (15  
169 female coalitions, 15 male coalitions Figure 2b). We programmed GPS satellite collars  
170 to record GPS locations at 17:00, 21:00, 01:00, 05:00, and 09:00 o'clock. The eight-hour  
171 window between 09:00 and 17:00 can be considered comparable to a four-hour window,  
172 as wild dogs generally rest between 11:00 and 15:00, leaving approximately four hours of  
173 activity (Hayward and Slotow, 2009). The collected GPS data was regularly transmitted to  
174 a base-station via Iridium satellite, thereby allowing dispersing individuals to be monitored,  
175 even if they ventured across national borders. In total, we obtained 5,940 locations during  
176 dispersal, with an average of  $198 \pm 239$  locations per coalition. Occasionally, the acquisition  
177 of a GPS location failed (success rate =  $93 \pm 8\%$ ), resulting in slight deviations from the  
178 aspired four-hourly schedule. Further details on the GPS collar fitting procedure and how  
179 we distinguished between dispersal and resident movements can be found in Cozzi et al.  
180 (2020) and Hofmann et al. (2021).

## 181 2.3 Covariates

182 We represented the physical landscape through which dispersers moved by a suite of spa-  
183 tial covariate layers known to influence wild dog movements during dispersal. We broadly  
184 categorized these spatial covariates into descriptors of (1) landscape characteristics, (2) cli-  
185 matic conditions, and (3) anthropogenic factors (Table 1) (see Hofmann et al., 2021, 2023).  
186 Besides spatial covariates, we also prepared a series of covariates relating to (4) light avail-  
187 ability (Table 1) (see Cozzi et al. 2012). To appropriately render seasonality in each of the  
188 spatial covariates (1-3), we downloaded them at the highest spatial and temporal resolu-  
189 tion available. That is, we obtained for each spatial covariate by a stack of raster layers  
190 that spanned the entire range of dates and locations for which we also collected GPS data  
191 of dispersing wild dogs. Depending on the covariate, this resulted in differing spatial and  
192 temporal resolutions (Table 1). Additionally, for each spatial covariate, we also generated a  
193 static layer, representing “average” conditions across the entire duration of the study. For  
194 this, we flattened each covariate stack into a single layer, thus removing seasonality from the

195 spatial data entirely. For continuous covariates, we achieved this by averaging conditions  
196 across all collected layers, whereas for categorical (binary) layers we identified areas that  
197 were covered by the respective category in at least 50% of all layers. Using the same aggrega-  
198 tion techniques, we computed covariate stacks representative of a typical year. That is,  
199 instead of removing seasonality by flattening across the entire range of dates, we flattened  
200 stacks across years, thereby eliminating year-specific effects. These final layers served to be  
201 used in the dispersal simulation, where we needed data representing seasonality in all covari-  
202 ates across a typical year. To summarize, we prepared each spatial covariate dynamically for  
203 the entire range of dates considered, dynamically for an average year, and statically across  
204 the entire range of dates considered.

### 205 2.3.1 Landscape Characteristics

206 We used data from the MODIS Vegetation Continuous Fields dataset (MOD44B V061;  
207 DiMiceli et al., 2022) to represent different vegetation types across the study area. The  
208 MOD44B dataset comprises three continuous layers, depicting the percentage cover of wood-  
209 land, shrubs/grassland, and bareland, respectively. The three layers added up to 100%, so  
210 we dropped bareland from further analysis, thus preventing perfect multi-collinearity. The  
211 MOD44B product is updated on day 65 of each year, so we used the R-package **RGISTools**  
212 (Pérez-Goya et al., 2020) to download yearly updated layers, each at a resolution of 250m x  
213 250m. We also obtained information on the normalized vegetation difference index (NDVI)  
214 through the MODIS MOD13Q1 dataset (Didan, 2015), which also has a resolution of 250m  
215 x 250m. This product is updated every 16 days, and we accessed the respective data through  
216 Google Earth Engine (Gorelick et al., 2017) using the R-package **rgee** (Aybar et al., 2024).  
217 To depict large, permanent water-bodies, we employed the Globeland30 dataset, from which  
218 we only retained the land-cover class water, while setting all other categories to dryland.  
219 Similarly, we used the MERIT Hydro dataset to obtain information on permanent rivers  
220 (Yamazaki et al., 2019). To dynamically render large water-bodies, particularly the flood-  
221 waters of the Okavango Delta, we prepared weekly updated floodmaps using remote sensed  
222 MODIS MOD43A4 satellite images. The underlying floodmapping algorithm is described in  
223 detail in Wolski et al. (2017) and Hofmann et al. (2021) and is implemented in the **floodmapr**  
224 package (available on GitHub; <https://github.com/DavidDHofmann/floodmapr>). To gen-  
225 erate a single layer representing major water bodies, we combined the water, river, and flood  
226 layers into a single stack with a resolution of 500m x 500m. Finally, we employed remote  
227 sensing to detect small, ephemeral water bodies (i.e., pans) using a custom random-forest

228 classifier applied to Sentinel 2 satellite imagery (European Space Agency, 2018; details of  
229 the classifier in Appendix A1). Sentinel 2 has a resolution of 10m and is therefore partic-  
230 ularly useful for obtaining information on small landscape features. Even though Sentinel  
231 2 satellite imagery is updated every 5 days, cloud cover often prohibited the computation  
232 of a “pan-map”. Consequently, we settled for monthly updated composite images, which  
233 effectively alleviated problems due to cloud cover. In summary, we produced one stack of  
234 layers representing major water bodies, and another stack of layers representing ephemeral  
235 water bodies. For both, we also computed corresponding distance-to stacks.

### 236 **2.3.2 Climate Descriptors**

237 We obtained hourly updated spatial layers on 2m above-ground temperature from the ERA5-  
238 Land dataset (Muñoz-Sabater et al., 2021) and hourly updated precipitation estimates from  
239 the Global Satellite Mapping of Precipitation dataset (Kubota et al., 2020). Both datasets  
240 were accessed and downloaded through Google Earth Engine (Gorelick et al., 2017) using  
241 the `rgee` package (Aybar et al., 2024) and had a resolution of 10km x 10km. To match  
242 hourly temperature and precipitation values with the four-hourly data collected by the GPS  
243 satellite collars fitted on the dispersing wild dogs, we computed average precipitation and  
244 temperature values over four hourly periods that matched the GPS collection schedule.

### 245 **2.3.3 Anthropogenic Features**

246 We combined information on human density, agricultural activities, and roads into a single  
247 proxy, which we generically termed human influence. We sourced information on human  
248 density from Facebook’s high resolution human density dataset (Tiecke et al., 2017), which  
249 we downloaded from the humdata website ([www.data.humdata.org/](http://www.data.humdata.org/)). We obtained infor-  
250 mation on the presence of agricultural fields from the Globeland30 (Chen et al., 2015) and  
251 Cropland (Xiong et al., 2017) datasets. We downloaded shapefiles comprising main tar-  
252 roads from OpenStreetMaps (OpenStreetMap contributors, 2017). Ultimately, we merged  
253 all anthropogenic features into a single layer (details in Hofmann et al., 2021) that had a  
254 resolution of 250m x 250m.

### 255 **2.3.4 Light Availability**

256 We computed light statistics using the `suncalc` and `moonlit` R-packages (Thieurmel and El-  
257 marhraoui, 2022; Šmielak, 2023) for the central coordinates of our study area at a 5-minute  
258 temporal resolution. The set of light statistics comprised a binary variable separating day

and night (i.e., sun < -18 °below the horizon) and a continuous estimate of moonlight illumination (relative to the maximum moon illumination). Based on those covariates, we generated a binary covariate separating bright from dark conditions. To provide a general understanding of this variable, bright conditions encompassed all daytime hours and those nighttime periods during which the moon was present in the sky and illuminated by approximately one-fourth; conversely, dark conditions included nighttime periods during which the moon was absent from the sky or present or was only minimally illuminated (further details in Appendices A2 and A3).

## 2.4 Step-Selection Models

We modeled habitat selection and movement behavior of dispersing wild dogs using integrated step-selection functions (iSSFs, Fortin et al., 2005; Avgar et al., 2016), following the procedure described in Muff et al. (2020). For this, we identified bursts of subsequent GPS locations where the duration between two GPS locations did not exceed 4 hours ( $\pm 15$  minutes) or 8 hours ( $\pm 30$  minutes, for data recorded between 09:00 and 17:00). Within each burst, we converted locations into steps, where a step represented the straight line segment between two consecutive locations (Turchin, 1998). For each step, we computed the associated step length (sl, in meters) and relative turning angle (ta, in radians). After this pre-processing, a total of 26 dispersing coalitions (12 female coalitions, 14 male coalitions) remained for further analyses. The final dataset comprised 5'310 steps ( $204 \pm 225$  per coalition), which we further categorized into wet (15 October to 15 April) and dry (15 April to 15 October) season, resulting in 3,124 steps (59%) during the dry season and 2,186 steps (41%) during the wet season.

We paired each *observed* step with a set of 100 *random* steps, generated by sampling turning angles from a uniform distribution  $U(-\pi, +\pi)$  and step lengths from a gamma distribution fitted to observed steps (scale  $\theta = 6.34$  and shape  $k = 0.39$ ). Together, an observed step and its associated random steps formed a stratum that received a unique identifier. Along each step, we extracted covariate values from the underlying spatial habitat layers, and we assigned the appropriate light conditions (Table 1). We opted for covariate extraction *along* steps rather than *at their endpoints*, as we believed that environmental conditions along steps were relevant in determining wild dog movement. For continuous covariates, we computed average values along each step, for categorical covariates the percentage cover of each category along the step. To model a decreasing marginal impact of “distance to” variables, we included their square-root as predictors in the final models. To facilitate model

292 convergence, we normalized extracted values to a range between 0 and 1.

293 To estimate habitat and movement parameters of interest, we applied the maximum likelihood procedure proposed by Muff et al. (2020), using the `glmmTMB` package (Brooks et al., 294 2017). Our model formula was based on knowledge from previous studies on dispersing wild 295 dogs (Hofmann et al., 2021, 2023) and comprised a movement kernel (describing movement 296 preferences), a habitat-selection function (describing habitat preferences) and their interactions 297 (describing how movement differs depending on habitat conditions). Notably, we 298 included descriptors of the step length and turning angle (`sl`, `log(sl)`, and `cos(ta)`) in the 299 regression model (Avgar et al., 2017; Fieberg et al., 2021). We also fitted a stratum-specific 300 intercept with a large fixed variance ( $10^6$ , Muff et al., 2020), and used dispersing coalition ID 301 to model random slopes. To examine whether the effect of accounting seasonality differed 302 depending on the employed model, we fit models either *excluding* interactions (hereafter 303 called simple model) or *including* interactions (hereafter called full model). Specifically, 304 in the simple model we only included covariates relating to landscape characteristics and 305 anthropogenic features in the simple model, as well as the step-descriptors mandatory for 306 conducting an iSSF (i.e., `sl`, `log(sl)`, and `cos(ta)`; Avgar et al., 2016). In the full model, 307 however, we included additional interactions with climatic descriptors and light conditions, 308 rendering that wild dog dispersal behavior may vary depending on those. As such, the structure 309 of the simple model can be viewed as a model structure that is usually employed in 310 permeability-based studies, which are restricted to spatial covariates. The model structure 311 of the full model, conversely, included additional complexities that can only be accounted 312 for when investigating connectivity vis IBMMs. To ensure comparability among each of the 313 six configurations presented in our framework, we employed the same models across all of 314 them. Specifically, we fitted models that differed in their degree of dynamism (Figure 1a). 315 Models one and two were fit using static covariates (Figure 1a, Stage 1), with model one 316 being a single-season model and model two being a multi-season model (wet vs. dry, Figure 317 1a, Stage 2). Models two and three, by contrast, were fit using dynamic covariates, with 318 model three being a single-season model, and model four being a multi-season model (wet 319 vs. dry, Figure 1a, Stage 2). To quantify how many random steps were necessary before 320 model estimates stabilized (sensu Fieberg et al., 2021), we fitted each model with 5, 10, 25, 321 50, 75, and 100 random steps.

323 **2.5 Validation**

324 We compared the predictive efficacy of each of the six configurations (Figure 1b) using  
325 k-fold cross-validation for case-control studies (Fortin et al., 2009). For this, we split the  
326 data into training and validation sets using an 80:20 ratio and fitted the four iSSF models  
327 described above. We then used the  $\beta$ -estimates to predict the probability of each random  
328 and observed step in the validation set for being chosen. Depending on the configuration,  
329 we predicted step-probabilities using static or dynamic covariates. Within each stratum,  
330 we assigned ranks 1-101 to each step based on predicted probabilities and recorded the  
331 number of times the observed step was assigned each rank. Finally, we computed Spearman's  
332 rank correlation between ranks and associated frequencies  $r_{s,realized}$ . The better a model's  
333 predictive ability, the more negative  $r_{s,realized}$  should be (i.e., the less often the observed step  
334 should be assigned a low rank). For reference, we also computed Spearman's rank correlation  
335 for randomized preferences ( $r_{s,random}$ ), which we achieved by removing the observed step  
336 from each stratum and identifying the rank of a randomly chosen step. We replicated this  
337 validation procedure 100 times and computed the mean correlation coefficient  $\bar{r}_{s,realized}$  and  
338  $\bar{r}_{random}$ , as well as their 95% percentiles across replicates. Ultimately, this validation proves  
339 a significant prediction in case the confidence intervals of  $\bar{r}_{s,realized}$  and  $\bar{r}_{s,random}$  do not  
340 overlap (Fortin et al., 2009).

341 **2.6 Simulations**

342 To assess differences in connectivity upon increasing seasonal dynamism, we ran dispersal  
343 simulations under the two most distinct configurations, i.e. the fully static (SSS, Figure 1)  
344 and fully dynamic (DMD, Figure 1) configurations. As source areas to initiate dispersers,  
345 we defined three distinct regions known to host viable wild dog populations (Figure 2). The  
346 definition of these areas was somewhat arbitrary, albeit we deliberately selected areas in  
347 the west and east of the Delta to examine potential influences of flooding on connectivity  
348 (Hofmann et al., 2024), as well as a more isolated location that was not influenced directly  
349 by the Delta's flood extent. To initiate simulated dispersal trajectories, we randomly placed  
350 1,000 start points within each of these source area, with start times that were equally  
351 distributed across the year. To simulate dispersal and obtain connectivity maps under both  
352 configurations, we applied the simulation algorithm for iSSFs described in Signer et al.  
353 (2017) and employed in Hofmann et al. (2023). A similar algorithm has recently been  
354 added to the `amt` R-package (Signer et al., 2024). We applied the simulation algorithm  
355 as follows. Originating from the start point, we generated a set of 25 random steps by

356 sampling step lengths from the fitted gamma distribution and turning angles from a uniform  
357 distribution. Along each random step, we extracted spatial covariates, computed relevant  
358 movement metrics (sl, log(sl), and cos(ta)), and assigned light conditions. We then employed  
359 the fitted iSSF model to predict the probability of each step for being chosen (i.e. the  
360 redistribution kernel). Based on assigned probabilities, we sampled one of the steps and  
361 updated the simulated individual's position and time. We repeated the procedure until a  
362 total of 2,000 steps were realized ( $\sim 400$  dispersal days).

363 Depending on the configuration, we employed different spatial covariates during the  
364 simulation. For the SMS configuration, we used the static set of covariates, which omitted  
365 any seasonality and assumed a static landscape over time. For the DMD configuration,  
366 on the other hand, we updated covariates dynamically as the simulated individuals moved.  
367 More specifically, we generated a new covariate stack after every simulated step, comprising  
368 spatial layers that best represented environmental conditions at that particular point in  
369 time (Figure 4). Note that we used the set of covariates representing an average year for  
370 this purpose. For both configurations, we ultimately obtained a heatmap (or utilization  
371 distribution) based on simulated trajectories. We also generated difference maps between  
372 the two configurations, highlighting areas where the difference in simulated connectivity  
373 were most pronounced.

### 374 3 Results

375 Due to convergence issues, we removed the covariates NDVI, precipitation, and distance to  
376 pans from all analyses. Some minor convergence issues remained and our validation proce-  
377 dure failed in 59 out of 1,800 validation attempts. Since failures occurred across different  
378 configurations and were not clustered around one specific configuration, we deemed their  
379 exclusion of no concern.

#### 380 3.1 Step-Selection Models

381 Patterns of habitat selection and movement behavior were qualitatively similar, irrespective  
382 of whether models were fit using static or dynamic covariates (Figure 5, Tables S3, S4, S5,  
383 S6) and irrespective of the number of considered random steps (Figure S9). The most notable  
384 quantitative difference when using static vs. dynamic covariates (see Figure 1a) was that  
385 models fitted using dynamic covariates resulted in narrower confidence intervals (Figure 5).  
386 Furthermore, effect sizes (i.e.,  $\beta$ -estimates) of models fit using static covariates were more  
387 pronounced than effect sizes from models that were fit using dynamic covariates (Figure 5).

388 Differences were most marked for  $\beta_{DistanceToWater^{0.5}}$ , which was estimated  $\approx -0.8$  using  
389 static covariates, but  $\approx -0.3$  when using dynamic covariates.

390 Differences in  $\beta$ -estimates between seasons were moderate and most pronounced when  
391 models were fit using static covariates. For instance, when models were fit using static co-  
392 variates,  $\beta_{Water}$  was  $\approx -1.1$  during the dry season but ( $\approx 0.2$  during the wet season). When  
393 dynamic covariates were used, by contrast,  $\beta_{Water}$  was ( $\approx -0.6$  and  $\approx -0.3$ ), respectively.  
394  $\beta_{sl:Dark}$  was also markedly lower during the wet season ( $\approx -0.9$ ), compared to the dry  
395 season ( $\approx -0.1$ ). Plots that aid with the interpretation of the resulting models are provided  
396 in Figure S10.

### 397 3.2 Validation

398 Spearman's rank correlation coefficients ( $r$ ) obtained from the validation procedure revealed  
399 that predictions from the full model performed better than those from the simple model  
400 ( $\bar{r}_{simple} = -0.5$ ,  $\bar{r}_{full} = -0.9$ , Figure 6). Irrespective of the employed model, Spearman's  
401 rank correlation differed significantly depending on the amount of dynamism considered  
402 (simple:  $F(5, 593) = 26.45$ ,  $p < 0.001$ , full:  $F(5, 594) = 7.14$ ,  $p < 0.001$ ), albeit with  
403 moderate effect sizes. In the simple model, moving from a fully static (SSS) to a fully  
404 dynamic (DMD) configuration decreased Spearmans's rank correlation (i.e., increased the  
405 predictive performance) by 0.15 from -0.41 to -0.56. In the full model, moving from a fully  
406 static (SSS) to a fully dynamic (DMD) configuration entailed an increase in  $r$  (i.e. a decrease  
407 in the predictive performance) from -0.89 to -0.88. This suggests that, our hypothesis that  
408 increased dynamism results in better predictive performance only holds with the simple  
409 model (Figure 6a), but not the full model (Figure 6b).

### 410 3.3 Simulations

411 Simulations under the most static (SSS) and dynamic (DMD) configurations revealed dif-  
412 ferent connectivity patterns (Figure 7). In the static configuration, simulated dispersal  
413 trajectories more concentrated, resulting in frequent movement across a few key habitats.  
414 In the dynamic configuration, by contrast, simulated trajectories were more homogeneously  
415 distributed. Qualitatively, connectivity patterns appeared similar between the simple and  
416 full models. Given the similarities in habitat selection emerging under the two models, this  
417 was to be expected.

418 **4 Discussion**

419 **4.1 Brief Summary**

420 We introduced a framework to highlight that seasonality can enter a connectivity analy-  
421 sis at three distinct stages; (1) when extracting spatial covariates for fitting the selection  
422 model, (2) when fitting the selection model, and (3) when predicting from the fitted model.  
423 Through combination, this yields six configurations that differ in their degree of dynamism  
424 and, arguably, realism. We fitted the models associated with each configuration using GPS  
425 data on dispersing wild dogs and iSSFs and employed a rigorous validation procedure to  
426 investigate potential gains in predictive performance that can be reaped by incorporating  
427 different levels of dynamism. Results from the fitted models showed that including sea-  
428 sonality only marginally affected the inferred patterns of habitat selection and movement  
429 behavior. Similarly, the validation procedure suggested only moderate improvements in  
430 predictive performance upon increasing the degree of dynamism. Crucially, these benefits  
431 were limited to an overly simplistic model and vanished upon fitting a more complex one.  
432 We therefore could not pinpoint a specific stage at which including seasonality was particu-  
433 larly beneficial. Despite this, we found that dispersal simulations under the most static and  
434 most dynamic configurations resulted in differing connectivity patterns. Under the most  
435 static configuration, landscape connectivity was clumped around a few hot spots, whereas it  
436 was homogeneously distributed across the landscape under the most dynamic configuration.  
437 Finally, our work demonstrated that simulations from IBMMs effectively allow rendering  
438 seasonal changes in the landscape, achieving a degree of seasonal dynamism and realism  
439 that cannot be reached using permeability-based connectivity models.

440 **4.2 Moderate Improvements upon Increasing Dynamism**

441 Our validation procedure revealed only moderate improvements in our ability to predict  
442 dispersal movements when increasing the degree of dynamism. Given the system's extreme  
443 seasonal variability, this was somewhat surprising. We believe that the absence of a more  
444 pronounced improvement can be traced back to multiple factors. Firstly, we focused our  
445 analysis on dispersing individuals, which cover large distances in search of potential mates  
446 and a suitable territory (McNutt, 1996; Cozzi et al., 2020). In our case, the average 4-hourly  
447 step length was 2.5 km, suggesting that dispersers cross and sample numerous unfamiliar  
448 areas and potentially unsuitable habitats within short time. We thus hypothesize that the  
449 spatial scale at which seasonality affects environmental characteristics did not suffice to

match the spatial scale at which our focal species perceives and moves across the landscape during dispersal. A further explanation could be that dispersing individuals prioritize finding unoccupied territories or areas with low competition, rather than focusing on specific habitat types (e.g., Creel and Creel, 1996; Creel, 2001). Dispersers' habitat selection may therefore be more strongly influenced by territorial considerations (*sensu* Cozzi et al., 2018) and only little affected by seasonally changing landscape characteristics. This would also explain the relatively weak selection or avoidance of environmental characteristics exhibited in Figure 5. Finally, the AWD is a generalist species that can occupy a broad variety of habitats (Woodroffe and Donnelly, 2011). A certain tolerance towards changing environmental conditions can therefore be expected and may explain why seasonal differences were faint. This holds particularly true for dispersers, which are usually more tolerant towards unfavorable habitat conditions as they spend little time within the same area (O'Neill et al., 2020).

### 4.3 Substantial Improvements upon Fitting a Complex Model

In comparison to the improvements achieved by increasing dynamism, a more significant improvement in predictive ability was achieved by moving from the simple to the full iSSF model. In the full model, we included several interactions that accounted for wild dogs' biology, such as reduced movement during dark nights (Cozzi et al., 2013) or during times of high ambient temperature (Rabaiotti et al., 2021). Even though these interactions are not directly linked to connectivity, they clearly accounted for a substantial amount of variation in observed dispersal movements and facilitated predictions from the fitted model. We also allowed for potential changes in dispersers' movement behavior depending on habitat conditions, such as shorter steps in areas covered by water (Hofmann et al., 2023). Overall, the inclusion of these interactions elevated the predictive ability of our dispersal model to such a high level that increasing dynamism did not provide any further improvements. Notably, the ability of encapsulating such a detailed and mechanistic understanding of dispersal movements is unique to IBMMs and cannot be achieved using permeability-based connectivity models.

### 4.4 Dynamic Connectivity

When comparing connectivity under the most static (SSS) and dynamic (DMD) configurations, we observed that connectivity was clumped along a few major dispersal hotspots under the static configuration, but homogeneously distributed across the entire landscape under

the dynamic configuration. This corroborates previous research showing that static representations tend to result in an underestimation of connectivity because seasonal stepping stones or corridors are missed (Martensen et al., 2017). With the help of such seasonally-available dispersal habitats, areas that would otherwise be difficult to reach become accessible, even if only for a limited time. In our study, such stepping stones could arise in two ways. Firstly, the landscape could change seasonally, which may have shifted preferred habitats, leading to the emergence of alternative movement corridors. In addition, habitat or movement preferences of simulated individuals could change, resulting in different habitat characteristics being traversed depending on the season. In combination, varying landscape conditions and species preferences resulted in a more balanced mosaic of connectivity across the year. Importantly, the fact that connectivity is more evenly distributed across the year does not exclude the possibility that certain areas experience lower connectivity seasonally. As already shown by Osipova et al. (2019), a static representation may result in both an over- and under-estimation of short-term connectivity, depending on the area and season. For conservation planning, this implies a need to protect landscapes at broader scales, as areas that provide little connectivity during some season may become critical during others. A dynamic take at connectivity therefore improves our understanding of ecological processes in dynamic landscapes and may help to identify otherwise overlooked dispersal hotspots.

## 4.5 The Costs of Incorporating Dynamism

Increasing seasonal dynamism to model dynamic connectivity comes at significant costs, both in terms of data requirements and computational challenges. To represent seasonal changes in the landscape, one needs to download and process frequently updated spatial layers for each seasonal covariate. This is time-consuming and implies a substantial increase in the data-volume that needs to be handled. Because seasonal products are comparably rare, the choice to model connectivity dynamically will also entail a significant restriction in the number of potential covariates or require custom remote sensing algorithms (e.g., Appendix A1). Seasonal or remote sensed layers are also more susceptible to noise and missing values, particularly in cases where cloud cover is frequent. Extracting covariates from seasonal layers poses a further challenge, as data need to be extracted from those layers that best represent environmental conditions at the time of the respective observed or random step. This applies to the extraction of data for model fitting, as well as when extracting data during the simulation. Finally, splitting the species data by season to fit seasonal selection models significantly reduces the amount of data remaining per season, potentially causing

515 convergence issues. In our case, these additional efforts were not outweighed by an improved  
516 predictive ability. This finding is, however, likely highly specific to our study system. We  
517 therefore do not wish to discourage future studies from accounting for seasonality when  
518 assessing connectivity. Instead, we'd like to view our study as an example that the benefits  
519 of increased realism do not necessarily justify the additional complexity they bring about  
520 and that the associated costs and benefits need to be carefully pondered (Puy and Saltelli,  
521 2022).

## 522 4.6 Validation Procedure

523 Our validation procedure was focused on validation at the step level, but did not directly  
524 test how well predictions of functional connectivity agreed with true connectivity. This was  
525 owed to a conceptual limitation when trying to validate seasonal connectivity predicted from  
526 an IBMM. In seasonal landscapes, connectivity not only varies spatially, but also temporally.  
527 A meaningful validation therefore requires that connectivity is predicted separately for each  
528 timestamp in the validation data. In our case, for instance, the fact that the landscape  
529 was updated every 4 hours implies that a new connectivity map would need to be created  
530 around each validation step. This is equivalent to validating connectivity at the step level,  
531 which is why we deemed the application of k-fold cross-validation for case and control studies  
532 using Spearman's rank correlation as an appropriate validation technique. Note, however,  
533 that Spearman's rank correlation coefficient is heavily dependent on the number of steps  
534 per stratum and should therefore not be used to compare predictive efficacy across studies  
535 (Figure S11). For static connectivity analyses, alternative validation techniques exist. Mc-  
536 Clure et al. (2016), for instance, proposed a suite of validation metrics (applied in Zeller  
537 et al., 2018; Finerty et al., 2023). These largely work by comparing connectivity at ran-  
538 dom locations with connectivity at locations where the focal species was observed. Because  
539 these metrics fail to account for potential autocorrelation in the validation data (which is  
540 usually present in GPS data; (Otis and White, 1999)), Brennan et al. (2020) suggested val-  
541 idating connectivity by applying a path- or step-selection model to withheld data. If the  
542 fitted model proves significant selection towards areas of high connectivity, predictions are  
543 indeed indicative of functional connectivity (sensu Brennan et al., 2020). Developing similar  
544 approaches for dynamic connectivity analyses remains a task for future studies.

**545 4.7 Seasonal Habitat Selection**

**546** When we fit models assuming static covariates, wild dogs displayed a preference for areas  
**547** close to water, irrespective of the season. However, water itself appeared to be only avoided  
**548** during the dry season. This was likely caused by a misrepresentation of areas covered by  
**549** water in the static configuration. Since rainwater collected in Angola only slowly descents  
**550** through the Okavango Delta's tributaries (McCarthy et al., 1997), large portions of its  
**551** floodplains remain dry during the wet season McCarthy et al. (2003). On static covariates,  
**552** which represent average conditions across both seasons, it may appear as if individuals moved  
**553** through areas covered by water, albeit in reality they likely moved along them. Indeed, upon  
**554** accounting for such seasonal changes by considering seasonally updated covariate layers,  
**555** parameter estimates from the selection models assimilated and suggested avoidance of water  
**556** across both seasons. Our choice of splitting data into wet and dry season based on a fixed set  
**557** of dates can be viewed as a further limitation, as it assumes an immediate switch from one  
**558** season to another. In reality, season-transitions are not abrupt but rather gradual and their  
**559** timing may vary from year to year. A more robust approach would therefore be to define the  
**560** start and end of each season based on bio-climatic descriptors and to ignore data collected  
**561** during transitional periods. This may imply a loss of data, but could help to detect seasonal  
**562** selection patterns. In our case, retaining all data was necessary to ensure model convergence,  
**563** but may have resulted in a cross-contamination between seasons and therefore reduced our  
**564** ability to pick up seasonal differences in parameter estimates. Indeed, other studies reported  
**565** that habitat selection of their focal species varied greatly between seasons (but see Squires  
**566** et al., 2013). Benz et al. (2016), for instance, found that dispersing in elk (*Cervus elaphus*)  
**567** exhibit vastly different habitat preferences during winter and summer. Similarly, Osipova  
**568** et al. (2019) report that habitat selection of African elephants (*Loxodonta africana*) in South  
**569** Africa differs between the wet and dry season. The importance of seasonality thus appears  
**570** to be highly system dependent.

**571 4.8 Conclusion**

**572** In conclusion, we explored the importance of incorporating different degrees of dynamism  
**573** when studying dispersal and connectivity. Overall, our findings suggested only moderate  
**574** improvements in predictive performance upon increasing the level of dynamism. Neverthe-  
**575** less, connectivity patterns as inferred from simulated dispersal trajectories differed vastly,  
**576** with connectivity being more evenly distributed when seasonality was accounted for. While  
**577** increased realism via improved representation of seasonality may offer novel insights into

578 ecological processes, the benefits must be carefully weighed against the added complexity  
579 and effort required to collect seasonal data and model seasonal dynamism in the focal species'  
580 preferences. Moving forward, our study serves as an example that while accounting for sea-  
581 sonality could be crucial for some study systems, it may not always justify the additional  
582 complexity, emphasizing the need for thoughtful consideration of costs and benefits in future  
583 research.

## 584 **5 Authors' Contributions**

585 D.D.H. and G.C. conceived the study and designed methodology; D.D.H., G.C., D.M.B, and  
586 J.W.M. collected the data; D.D.H. analysed the data; G.C. assisted with modeling; D.D.H.  
587 and G.C. wrote the first draft of the manuscript and all authors contributed to the drafts  
588 at several stages and gave final approval for publication.

## 589 **6 Data Availability**

590 Access to R-scripts to replicate our analyses will be provided through an online repository  
591 at the time of publication.

## 592 **7 Acknowledgments & Funding**

593 We thank the Ministry of Environment and Tourism and the Department of Wildlife and  
594 National Parks of Botswana for granting permission to conduct this research. D.D.H. was  
595 funded by a Swiss National Science Foundation Grant No. 310030\_204478 to G.C.

**596 References**

- 597 Abrahms, B., Sawyer, S. C., Jordan, N. R., McNutt, J. W., Wilson, A. M., and Brashares,  
598 J. S. (2017). Does Wildlife Resource Selection Accurately Inform Corridor Conservation?  
599 *Journal of Applied Ecology*, 54(2):412–422.
- 600 Adriaensen, F., Chardon, J., De Blust, G., Swinnen, E., Villalba, S., Gulinck, H., and  
601 Matthysen, E. (2003). The Application of ‘Least-Cost’ Modelling as a Functional Land-  
602 scape Model. *Landscape and Urban Planning*, 64(4):233–247.
- 603 Allen, C. H., Parrott, L., and Kyle, C. (2016). An Individual-Based Modelling Approach to  
604 Estimate Landscape Connectivity for Bighorn Sheep (*Ovis canadensis*). *PeerJ*, 4:e2001.
- 605 Avgar, T., Lele, S. R., Keim, J. L., and Boyce, M. S. (2017). Relative Selection Strength:  
606 Quantifying Effect Size in Habitat- and Step-Selection Inference. *Ecology and Evolution*,  
607 7(14):5322–5330.
- 608 Avgar, T., Potts, J. R., Lewis, M. A., and Boyce, M. S. (2016). Integrated Step Selection  
609 Analysis: Bridging the Gap Between Resource Selection and Animal Movement. *Methods  
in Ecology and Evolution*, 7(5):619–630.
- 610 Aybar, C., Qiusheng, W., Bautista, L., Yali, R., Barja, A., Ushey, K., Ooms, J., Appelhans,  
611 T., Allaire, J. J., Tang, Y., Roy, S., Adaudo, M., Carrasco, G., Bengtsson, H., Hollister,  
612 J., Donchyts, G., and JOSS, M. (2024). Rgee: R Bindings for Calling the ‘Earth Engine’  
613 API.
- 614 Baddeley, A., Rubak, E., and Turner, R. (2015). *Spatial Point Patterns: Methodology and  
Applications with R*. Chapman and Hall/CRC Press, London.
- 615 Baguette, M., Blanchet, S., Legrand, D., Stevens, V. M., and Turlure, C. (2013). Indi-  
616 vidual Dispersal, Landscape Connectivity and Ecological Networks. *Biological Reviews*,  
617 88(2):310–326.
- 618 Baldwin, R. F., Calhoun, A. J. K., and deMaynadier, P. G. (2006). Conservation Planning  
619 for Amphibian Species with Complex Habitat Requirements: A Case Study Using Move-  
620 ments and Habitat Selection of the Wood Frog *Rana Sylvatica*. *Journal of Herpetology*,  
621 40(4):442–453.
- 622 Behr, D. M., McNutt, J. W., Ozgul, A., and Cozzi, G. (2020). When to Stay and When  
623 to Leave? Proximate Causes of Dispersal in an Endangered Social Carnivore. *Journal of  
Animal Ecology*, 89(10):2356–2366.
- 624 Benz, R. A., Boyce, M. S., Thurfjell, H., Paton, D. G., Musiani, M., Dormann, C. F., and  
625 Ciuti, S. (2016). Dispersal Ecology Informs Design of Large-Scale Wildlife Corridors.  
626 *PLoS ONE*, 11(9):e0162989.
- 627 Beyer, H. L., Haydon, D. T., Morales, J. M., Frair, J. L., Hebblewhite, M., Mitchell, M.,  
628 and Matthiopoulos, J. (2010). The Interpretation of Habitat Preference Metrics Under  
629 Use–Availability Designs. *Philosophical Transactions of the Royal Society B: Biological  
Sciences*, 365(1550):2245–2254.
- 630 Bishop-Taylor, R., Tulbure, M. G., and Broich, M. (2018). Evaluating Static and Dynamic  
631 Landscape Connectivity Modelling Using a 25-Year Remote Sensing Time Series. *Landscape  
632 Ecology*, 33(4):625–640.
- 633 Boyce, M. S., Vernier, P. R., Nielsen, S. E., and Schmiegelow, F. K. (2002). Evaluating  
634 Resource Selection Functions. *Ecological Modelling*, 157(2-3):281–300.
- 635 Brennan, A., Beytell, P., Aschenborn, O., Du Preez, P., Funston, P., Hanssen, L., Kilian,  
636 J., Stuart-Hill, G., Taylor, R., and Naidoo, R. (2020). Characterizing Multispecies Con-  
637 nectivity Across a Transfrontier Conservation Landscape. *Journal of Applied Ecology*,  
638 57(9):1700–1710.

- 643 Brooks, M. E., Kristensen, K., van Benthem, K. J., Magnusson, A., Berg, C. W., Nielsen,  
644 A., Skaug, H. J., Maechler, M., and Bolker, B. M. (2017). glmmTMB Balances Speed and  
645 Flexibility Among Packages for Zero-Inflated Generalized Linear Mixed Modeling. *The R  
646 Journal*, 9(2):378–400.
- 647 Chen, J., Chen, J., Liao, A., Cao, X., Chen, L., Chen, X., He, C., Han, G., Peng, S., and Lu,  
648 M. (2015). Global Land Cover Mapping at 30 m Resolution: A POK-Based Operational  
649 Approach. *ISPRS Journal of Photogrammetry and Remote Sensing*, 103:7–27.
- 650 Chetkiewicz, C.-L. B. and Boyce, M. S. (2009). Use of Resource Selection Functions to  
651 Identify Conservation Corridors. *Journal of Applied Ecology*, 46(5):1036–1047.
- 652 Ciudad, C., Mateo-Sánchez, M. C., Gastón, A., Blazquez-Cabrera, S., and Saura, S. (2021).  
653 Landscape Connectivity Estimates Are Affected by Spatial Resolution, Habitat Seasonal-  
654 ity and Population Trends. *Biodiversity and Conservation*, 30(5):1395–1413.
- 655 Cozzi, G., Behr, D. M., Webster, H. S., Claase, M., Bryce, C. M., Modise, B., McNutt, J. W.,  
656 and Ozgul, A. (2020). African Wild Dog Dispersal and Implications for Management. *The  
657 Journal of Wildlife Management*, 84(4):614–621.
- 658 Cozzi, G., Broekhuis, F., McNutt, J. W., and Schmid, B. (2013). Comparison of the Effects of  
659 Artificial and Natural Barriers on Large African Carnivores: Implications for Interspecific  
660 Relationships and Connectivity. *Journal of Animal Ecology*, 82(3):707–715.
- 661 Cozzi, G., Broekhuis, F., McNutt, J. W., Turnbull, L. A., Macdonald, D. W., and Schmid,  
662 B. (2012). Fear of the Dark or Dinner by Moonlight? Reduced Temporal Partitioning  
663 Among Africa's Large Carnivores. *Ecology*, 93(12):2590–2599.
- 664 Cozzi, G., Maag, N., Börger, L., Clutton-Brock, T. H., and Ozgul, A. (2018). Socially  
665 Informed Dispersal in a Territorial Cooperative Breeder. *Journal of Animal Ecology*,  
666 87(3):838–849.
- 667 Creel, S. (2001). Four Factors Modifying the Effect of Competition on Carnivore Population  
668 Dynamics as Illustrated by African Wild Dogs. *Conservation Biology*, 15(1):271–274.
- 669 Creel, S. and Creel, N. M. (1996). Limitation of African Wild Dogs by Competition with  
670 Larger Carnivores. *Conservation Biology*, 10(2):526–538.
- 671 Cushman, S. A. and Lewis, J. S. (2010). Movement Behavior Explains Genetic Differentiation  
672 in American Black Bears. *Landscape Ecology*, 25(10):1613–1625.
- 673 Davies-Mostert, H. T., Kamler, J. F., Mills, M. G. L., Jackson, C. R., Rasmussen, G. S. A.,  
674 Groom, R. J., and Macdonald, D. W. (2012). Long-Distance Transboundary Dispersal  
675 of African Wild Dogs Among Protected Areas in Southern Africa. *African Journal of  
676 Ecology*, 50(4):500–506.
- 677 Didan, K. (2015). MOD13Q1 Modis/Terra Vegetation Indices 16-Day L3 Global 250m Sin  
678 Grid V006.
- 679 DiMiceli, C., Sohlberg, R., and Townshend, J. (2022). MODIS/Terra Vegetation Continuous  
680 Fields Yearly L3 Global 250m SIN Grid V061.
- 681 Diniz, M. F., Cushman, S. A., Machado, R. B., and De Marco Júnior, P. (2019). Landscape  
682 Connectivity Modeling from the Perspective of Animal Dispersal. *Landscape Ecology*,  
683 35:41–58.
- 684 Doerr, V. A. J., Barrett, T., and Doerr, E. D. (2011). Connectivity, Dispersal Behaviour  
685 and Conservation Under Climate Change: A Response to Hodgson et al.: Connectivity  
686 and Dispersal Behaviour. *Journal of Applied Ecology*, 48(1):143–147.
- 687 Elliot, N. B., Cushman, S. A., Macdonald, D. W., and Loveridge, A. J. (2014). The Devil  
688 Is in the Dispersers: Predictions of Landscape Connectivity Change with Demography.  
689 *Journal of Applied Ecology*, 51(5):1169–1178.

- 690 European Space Agency (2018). Sentinel-2 MSI Level-2A BOA Reflectance.
- 691 Fahrig, L. (2003). Effects of Habitat Fragmentation on Biodiversity. *Annual Review of*  
692 *Ecology, Evolution, and Systematics*, 34(1):487–515.
- 693 Fattebert, J., Robinson, H. S., Balme, G., Slotow, R., and Hunter, L. (2015). Structural  
694 Habitat Predicts Functional Dispersal Habitat of a Large Carnivore: How Leopards  
695 Change Spots. *Ecological Applications*, 25(7):1911–1921.
- 696 Fieberg, J., Matthiopoulos, J., Hebblewhite, M., Boyce, M. S., and Frair, J. L. (2010).  
697 Correlation and Studies of Habitat Selection: Problem, Red Herring or Opportunity?  
698 *Philosophical Transactions of the Royal Society B: Biological Sciences*, 365(1550):2233–  
699 2244.
- 700 Fieberg, J., Signer, J., Smith, B., and Avgar, T. (2021). A ‘How to’ Guide for Interpreting  
701 Parameters in Habitat-Selection Analyses. *Journal of Animal Ecology*, 90(5):1027–1043.
- 702 Finerty, G. E., Cushman, S. A., Bauer, D. T., Elliot, N. B., Kesch, M. K., Macdonald,  
703 D. W., and Loveridge, A. J. (2023). Evaluating Connectivity Models for Conservation:  
704 Insights from African Lion Dispersal Patterns. *Landscape Ecology*, 38(12):3205–3219.
- 705 Fortin, D., Beyer, H. L., Boyce, M. S., Smith, D. W., Duchesne, T., and Mao, J. S. (2005).  
706 Wolves Influence Elk Movements: Behavior Shapes a Trophic Cascade in Yellowstone  
707 National Park. *Ecology*, 86(5):1320–1330.
- 708 Fortin, D., Fortin, M.-E., Beyer, H. L., Duchesne, T., Courant, S., and Dancose, K. (2009).  
709 Group-Size-Mediated Habitat Selection and Group Fusion–Fission Dynamics of Bison  
710 Under Predation Risk. *Ecology*, 90(9):2480–2490.
- 711 Frankham, R., Ballou, J. D., Briscoe, D. A., and McInnes, K. H. (2002). *Introduction to*  
712 *Conservation Genetics*. Cambridge University Press.
- 713 Gorelick, N., Hancher, M., Dixon, M., Ilyushchenko, S., Thau, D., and Moore, R. (2017).  
714 Google Earth Engine: Planetary-Scale Geospatial Analysis for Everyone. *Remote Sensing*  
715 *of Environment*.
- 716 Gumbrecht, T., Wolski, P., Frost, P., and McCarthy, T. (2004). Forecasting the Spatial  
717 Extent of the Annual Flood in the Okavango Delta, Botswana. *Journal of Hydrology*,  
718 290(3-4):178–191.
- 719 Hanski, I. (1999). *Metapopulation Ecology*. Oxford University Press.
- 720 Hauenstein, S., Fattebert, J., Grüebler, M. U., Naef-Daenzer, B., Pe'er, G., and Hartig, F.  
721 (2019). Calibrating an Individual-Based Movement Model to Predict Functional Connec-  
722 tivity for Little Owls. *Ecological Applications*, 29(4):e01873.
- 723 Hayward, M. W. and Slotow, R. (2009). Temporal Partitioning of Activity in Large African  
724 Carnivores: Tests of Multiple Hypotheses. *South African Journal of Wildlife Research*,  
725 39(2):109–125.
- 726 Heller, N. E. and Zavaleta, E. S. (2009). Biodiversity Management in the Face of Climate  
727 Change: A Review of 22 Years of Recommendations. *Biological Conservation*, 142(1):14–  
728 32.
- 729 Hijmans, R. J., Bivand, R., Pebesma, E., and Sumner, M. D. (2024). Terra: Spatial Data  
730 Analysis.
- 731 Hofmann, D. D., Behr, D. M., McNutt, J. W., Ozgul, A., and Cozzi, G. (2021). Bound  
732 Within Boundaries: Do Protected Areas Cover Movement Corridors of Their Most Mobile,  
733 Protected Species? *Journal of Applied Ecology*, 58(6):1133–1144.
- 734 Hofmann, D. D., Behr, D. M., McNutt, J. W., Ozgul, A., and Cozzi, G. (2024). Dispersal  
735 and Connectivity in Increasingly Extreme Climatic Conditions. *Global Change Biology*.

- 736 Hofmann, D. D., Cozzi, G., McNutt, J. W., Ozgul, A., and Behr, D. M. (2023). A Three-  
 737 Step Approach for Assessing Landscape Connectivity Via Simulated Dispersal: African  
 738 Wild Dog Case Study. *Landscape Ecology*, 38(4):981–998.
- 739 Kanagaraj, R., Wiegand, T., Kramer-Schadt, S., and Goyal, S. P. (2013). Using Individual-  
 740 Based Movement Models to Assess Inter-Patch Connectivity for Large Carnivores in Frag-  
 741 mented Landscapes. *Biological Conservation*, 167:298–309.
- 742 Kassambara, A. (2024). Ggpubr: 'ggplot2' Based Publication Ready Plots.
- 743 Kaszta, Ź., Cushman, S. A., and Slotow, R. (2021). Temporal Non-Stationarity of Path-  
 744 Selection Movement Models and Connectivity: An Example of African Elephants in  
 745 Kruger National Park. *Frontiers in Ecology and Evolution*, 9:553263.
- 746 Keeley, A. T. H., Beier, P., Creech, T., Jones, K., Jongman, R. H., Stonecipher, G., and Ta-  
 747 bor, G. M. (2019). Thirty Years of Connectivity Conservation Planning: An Assessment of  
 748 Factors Influencing Plan Implementation. *Environmental Research Letters*, 14(10):103001.
- 749 Kubota, T., Aonashi, K., Ushio, T., Shige, S., Takayabu, Y. N., Kachi, M., Arai, Y.,  
 750 Tashima, T., Masaki, T., Kawamoto, N., Mega, T., Yamamoto, M. K., Hamada, A., Ya-  
 751 maji, M., Liu, G., and Oki, R. (2020). Global Satellite Mapping of Precipitation (GSMaP)  
 752 Products in the GPM Era. In Levizzani, V., Kidd, C., Kirschbaum, D. B., Kummerow,  
 753 C. D., Nakamura, K., and Turk, F. J., editors, *Satellite Precipitation Measurement: Vol-*  
 754 *ume 1*, Advances in Global Change Research, pages 355–373. Springer International Pub-  
 755 lishing, Cham.
- 756 MacArthur, R. H. and Wilson, E. O. (2001). *The Theory of Island Biogeography*. Princeton  
 757 University Press.
- 758 Manly, B. F., McDonald, L., Thomas, D. L., McDonald, T. L., and Erickson, W. P. (2007).  
 759 *Resource Selection by Animals: Statistical Design and Analysis for Field Studies*. Springer  
 760 Science & Business Media.
- 761 Martensen, A. C., Saura, S., and Fortin, M.-J. (2017). Spatio-Temporal Connectivity: As-  
 762 sessing the Amount of Reachable Habitat in Dynamic Landscapes. *Methods in Ecology*  
 763 *and Evolution*, 8(10):1253–1264.
- 764 Masenga, E. H., Jackson, C. R., Mjingo, E. E., Jacobson, A., Riggio, J., Lyamuya, R. D.,  
 765 Fyumagwa, R. D., Borner, M., and Røskraft, E. (2016). Insights into Long-Distance Dis-  
 766 persal by African Wild Dogs in East Africa. *African Journal of Ecology*, 54(1):95–98.
- 767 McCarthy, J. M., Gumbrecht, T., McCarthy, T., Frost, P., Wessels, K., and Seidel, F. (2003).  
 768 Flooding Patterns of the Okavango Wetland in Botswana between 1972 and 2000. *AMBIO: A Journal of the Human Environment*, 32(7):453–457.
- 770 McCarthy, T., Barry, M., Bloem, A., Ellery, W., Heister, H., Merry, C., Röther, H., and  
 771 Sternberg, H. (1997). The Gradient of the Okavango Fan, Botswana, and Its Sedimento-  
 772 logical and Tectonic Implications. *Journal of African Earth Sciences*, 24(1-2):65–78.
- 773 McClure, M. L., Hansen, A. J., and Inman, R. M. (2016). Connecting Models to Movements:  
 774 Testing Connectivity Model Predictions Against Empirical Migration and Dispersal Data.  
 775 *Landscape Ecology*, 31(7):1419–1432.
- 776 McNutt, J. W. (1996). Sex-Biased Dispersal in African Wild Dogs, *Lycaon pictus*. *Animal Behaviour*, 52(6):1067–1077.
- 778 McRae, B. H., Dickson, B. G., Keitt, T. H., and Shah, V. B. (2008). Using Circuit Theory to  
 779 Model Connectivity in Ecology, Evolution, and Conservation. *Ecology*, 89(10):2712–2724.
- 780 Mendelsohn, J. M., Vander Post, C., Ramberg, L., Murray-Hudson, M., Wolski, P., and  
 781 Mosepele, K. (2010). *Okavango Delta: Floods of Life*. RAISON, Windhoek, Namibia.

- 782 Merkle, J. A., Monteith, K. L., Aikens, E. O., Hayes, M. M., Hersey, K. R., Middleton,  
783 A. D., Oates, B. A., Sawyer, H., Scurlock, B. M., and Kauffman, M. J. (2016). Large  
784 Herbivores Surf Waves of Green-up During Spring. *Proceedings of the Royal Society B:  
785 Biological Sciences*, 283(1833):20160456.
- 786 Muñoz-Sabater, J., Dutra, E., Agustí-Panareda, A., Albergel, C., Arduini, G., Balsamo,  
787 G., Boussetta, S., Choulga, M., Harrigan, S., and Hersbach, H. (2021). ERA5-Land:  
788 A state-of-the-art global reanalysis dataset for land applications. *Earth System Science  
789 Data*, 13(9):4349–4383.
- 790 Muff, S., Signer, J., and Fieberg, J. (2020). Accounting for Individual-Specific Variation in  
791 Habitat-Selection Studies: Efficient Estimation of Mixed-Effects Models Using Bayesian  
792 or Frequentist Computation. *Journal of Animal Ecology*, 89(1):80–92.
- 793 Mui, A. B., Caverhill, B., Johnson, B., Fortin, M.-J., and He, Y. (2017). Using Multiple  
794 Metrics to Estimate Seasonal Landscape Connectivity for Blanding’s Turtles (*Emydoidea  
795 blandingsii*) in a Fragmented Landscape. *Landscape Ecology*, 32(3):531–546.
- 796 Naidoo, R., Chase, M. J., Beytell, P., Du Preez, P., Landen, K., Stuart-Hill, G., and Taylor,  
797 R. (2016). A Newly Discovered Wildlife Migration in Namibia and Botswana Is the  
798 Longest in Africa. *Oryx*, 50(1):138–146.
- 799 O’Neill, H. M. K., Durant, S. M., and Woodroffe, R. (2020). What Wild Dogs Want: Habitat  
800 Selection Differs Across Life Stages and Orders of Selection in a Wide-Ranging Carnivore.  
801 *BMC Zoology*, 5(1).
- 802 OpenStreetMap contributors (2017). Planet dump retrieved from <https://planet.osm.org>.
- 803 Osipova, L., Okello, M. M., Njumbi, S. J., Ngene, S., Western, D., Hayward, M. W., and  
804 Balkenhol, N. (2019). Using Step-Selection Functions to Model Landscape Connectivity  
805 for African Elephants: Accounting for Variability Across Individuals and Seasons. *Animal  
806 Conservation*, 22(1):35–48.
- 807 Otis, D. L. and White, G. C. (1999). Autocorrelation of Location Estimates and the Analysis  
808 of Radiotracking Data. *The Journal of Wildlife Management*, 63(3):1039–1044.
- 809 Pérez-Goya, U., Montesino-SanMartin, M., Militino, A. F., and Ugarte, M. D. (2020). RGIS-  
810 Tools: Downloading, Customizing, and Processing Time Series of Remote Sensing Data  
811 in R.
- 812 Perrin, N. and Mazalov, V. (2000). Local Competition, Inbreeding, and the Evolution of  
813 Sex-Biased Dispersal. *The American Naturalist*, 155(1):116–127.
- 814 Puy, A. and Saltelli, A. (2022). Mind the Hubris: Complexity Can Misfire.
- 815 R Core Team (2023). *R: A Language and Environment for Statistical Computing*. R Foun-  
816 dation for Statistical Computing, Vienna, Austria.
- 817 Rabaiotti, D., Groom, R., McNutt, J. W., Watermeyer, J., O’Neill, H. M. K., and Woodroffe,  
818 R. (2021). High Temperatures and Human Pressures Interact to Influence Mortality in  
819 an African Carnivore. *Ecology and Evolution*, 11(13):8495–8506.
- 820 Rabaiotti, D. and Woodroffe, R. (2019). Coping with Climate Change: Limited Behavioral  
821 Responses to Hot Weather in a Tropical Carnivore. *Oecologia*, 189(3):587–599.
- 822 Ramberg, L., Hancock, P., Lindholm, M., Meyer, T., Ringrose, S., Sliva, J., Van As, J.,  
823 and Vander Post, C. (2006). Species Diversity of the Okavango Delta, Botswana. *Aquatic  
824 Sciences*, 68(3):310–337.
- 825 Rasmussen, G. S. A. and Macdonald, D. W. (2012). Masking of the Zeitgeber: African Wild  
826 Dogs Mitigate Persecution by Balancing Time. *Journal of Zoology*, 286(3):232–242.

- 827 Rudnick, D. A., Ryan, S. J., Beier, P., Cushman, S. A., Dieffenbach, F., Epps, C. W.,  
828 Gerber, L. R., Hartter, J., Jenness, J. S., Kintsch, J., Merenlender, A. M., Perkl, R. M.,  
829 Preziosi, D. V., and Trombulak, S. C. (2012). The Role of Landscape Connectivity in  
830 Planning and Implementing Conservation and Restoration Priorities. *Issues in Ecology*,  
831 (16):1–23.
- 832 Rumiano, F., Wielgus, E., Miguel, E., Chamaillé-Jammes, S., Valls-Fox, H., Cornélis, D.,  
833 Garine-Wichatitsky, M. D., Fritz, H., Caron, A., and Tran, A. (2020). Remote Sensing  
834 of Environmental Drivers Influencing the Movement Ecology of Sympatric Wild and  
835 Domestic Ungulates in Semi-Arid Savannas, a Review. *Remote Sensing*, 12(19):3218.
- 836 Sandoval-Seres, E., Moyo, W., Madhlamoto, D., Madzikanda, H., Blinston, P., Kotze, R.,  
837 Van Der Meer, E., and Loveridge, A. (2022). Long-Distance African Wild Dog Dispersal  
838 Within the Kavango-Zambezi Transfrontier Conservation Area. *African Journal of  
839 Ecology*, 60(4):1262–1266.
- 840 Serneels, S. and Lambin, E. F. (2001). Impact of Land-Use Changes on the Wildebeest Mi-  
841 gration in the Northern Part of the Serengeti–Mara Ecosystem. *Journal of Biogeography*,  
842 28(3):391–407.
- 843 Signer, J., Fieberg, J., and Avgar, T. (2017). Estimating Utilization Distributions from  
844 Fitted Step-Selection Functions. *Ecosphere*, 8(4):e01771.
- 845 Signer, J., Fieberg, J., Reineking, B., Schlägel, U. E., Smith, B. J., Balkenhol, N., and  
846 Avgar, T. (2024). Simulating Animal Space Use from Fitted Integrated Step-Selection  
847 Functions. *Methods in Ecology and Evolution*, 15(1):43–50.
- 848 Simpkins, C. E. and Perry, G. L. (2017). Understanding the Impacts of Temporal Variability  
849 on Estimates of Landscape Connectivity. *Ecological Indicators*, 83:243–248.
- 850 Šmielak, M. K. (2023). Biologically Meaningful Moonlight Measures and Their Application  
851 in Ecological Research. *Behavioral Ecology and Sociobiology*, 77(2):21.
- 852 Squires, J. R., DeCesare, N. J., Olson, L. E., Kolbe, J. A., Hebblewhite, M., and Parks, S. A.  
853 (2013). Combining Resource Selection and Movement Behavior to Predict Corridors for  
854 Canada Lynx at Their Southern Range Periphery. *Biological Conservation*, 157:187–195.
- 855 Taylor, P. D., Fahrig, L., Henein, K., and Merriam, G. (1993). Connectivity Is a Vital  
856 Element of Landscape Structure. *Oikos*, 68(3):571–573.
- 857 Thieurmel, B. and Elmarhraoui, A. (2022). *Suncalc: Compute Sun Position, Sunlight  
858 Phases, Moon Position and Lunar Phase*.
- 859 Thurfjell, H., Ciuti, S., and Boyce, M. S. (2014). Applications of Step-Selection Functions  
860 in Ecology and Conservation. *Movement Ecology*, 2(1):4.
- 861 Tiecke, T. G., Liu, X., Zhang, A., Gros, A., Li, N., Yetman, G., Kilic, T., Murray, S.,  
862 Blanckespoor, B., Prydz, E. B., and Dang, H.-A. H. (2017). Mapping the World Population  
863 One Building at a Time.
- 864 Toth, C. and Józków, G. (2016). Remote Sensing Platforms and Sensors: A Survey. *ISPRS  
865 Journal of Photogrammetry and Remote Sensing*, 115:22–36.
- 866 Turchin, P. (1998). *Quantitative Analysis of Movement: Measuring and Modeling Population  
867 Redistribution in Animals and Plants*. Sinauer Associates, Sunderland, Mass.
- 868 Unnithan Kumar, S., Kaszta, Ź., and Cushman, S. A. (2022a). Pathwalker: A New  
869 Individual-Based Movement Model for Conservation Science and Connectivity Modelling.  
870 *ISPRS International Journal of Geo-Information*, 11(6):329.
- 871 Unnithan Kumar, S., Turnbull, J., Hartman Davies, O., Hodgetts, T., and Cushman, S. A.  
872 (2022b). Moving Beyond Landscape Resistance: Considerations for the Future of Con-  
873 nectivity Modelling and Conservation Science. *Landscape Ecology*, 37(10):2465–2480.

- 874 Vasudev, D., Fletcher, R. J., Goswami, V. R., and Krishnadas, M. (2015). From Disper-  
875 sal Constraints to Landscape Connectivity: Lessons from Species Distribution Modeling.  
876 *Ecography*, 38(10):967–978.
- 877 Wickham, H., Chang, W., Henry, L., Pedersen, T. L., Takahashi, K., Wilke, C., Woo, K.,  
878 Yutani, H., Dunnington, D., Posit, and PBC (2024). Ggplot2: Create Elegant Data  
879 Visualisations Using the Grammar of Graphics.
- 880 Wilson, B. H. and Dincer, T. (1976). An Introduction to the Hydrology and Hydrography of  
881 the Okavango Delta. Presented at the Symposium on the Okavango Delta and Its Future  
882 Utilization; Gaborone (Botswana); 30 Aug 1976. In *Proceedings of the Symposium on the  
883 Okavango Delta and Its Future Utilization, Barone, Botswana*.
- 884 Wolski, P., Murray-Hudson, M., Thito, K., and Cassidy, L. (2017). Keeping It Simple:  
885 Monitoring Flood Extent in Large Data-Poor Wetlands Using MODIS SWIR Data. *Interna-*  
886 *tional Journal of Applied Earth Observation and Geoinformation*, 57:224–234.
- 887 Wood, S. N. (2011). Fast Stable Restricted Maximum Likelihood and Marginal Likelihood  
888 Estimation of Semiparametric Generalized Linear Models. *Journal of the Royal Statistical  
889 Society Series B: Statistical Methodology*, 73(1):3–36.
- 890 Woodroffe, R. and Donnelly, C. A. (2011). Risk of Contact Between Endangered African  
891 Wild Dogs *Lycaon pictus* and Domestic Dogs: Opportunities for Pathogen Transmission.  
892 *Journal of Applied Ecology*, 48(6):1345–1354.
- 893 Woodroffe, R., Rabaiotti, D., Ngatia, D. K., Smallwood, T. R. C., Strelbel, S., and O'Neill,  
894 H. M. K. (2020). Dispersal Behaviour of African Wild Dogs in Kenya. *African Journal  
895 of Ecology*, 58(1):46–57.
- 896 Xiong, J., Thenkabail, P., Tilton, J., Gumma, M., Teluguntla, P., Oliphant, A., Congalton,  
897 R., Yadav, K., and Gorelick, N. (2017). Nominal 30-m Cropland Extent Map of Conti-  
898 nental Africa by Integrating Pixel-Based and Object-Based Algorithms Using Sentinel-2  
899 and Landsat-8 Data on Google Earth Engine. *Remote Sensing*, 9(10):1065.
- 900 Yamazaki, D., Ikeshima, D., Sosa, J., Bates, P. D., Allen, G., and Pavelsky, T. (2019).  
901 MERIT HYDRO: A High-Resolution Global Hydrography Map Based on Latest Topog-  
902 raphy Datasets. *Water Resources Research*.
- 903 Zeller, K., Lewison, R., Fletcher, R., Tulbure, M., and Jennings, M. (2020a). Understanding  
904 the Importance of Dynamic Landscape Connectivity. *Land*, 9(9):303.
- 905 Zeller, K. A., Jennings, M. K., Vickers, T. W., Ernest, H. B., Cushman, S. A., and Boyce,  
906 W. M. (2018). Are All Data Types and Connectivity Models Created Equal? Validating  
907 Common Connectivity Approaches with Dispersal Data. *Diversity and Distributions*,  
908 24(7):868–879.
- 909 Zeller, K. A., McGarigal, K., and Whiteley, A. R. (2012). Estimating Landscape Resistance  
910 to Movement: A Review. *Landscape Ecology*, 27(6):777–797.
- 911 Zeller, K. A., Wattles, D. W., Bauder, J. M., and DeStefano, S. (2020b). Forecasting  
912 Seasonal Habitat Connectivity in a Developing Landscape. *Land*, 9(7):233.

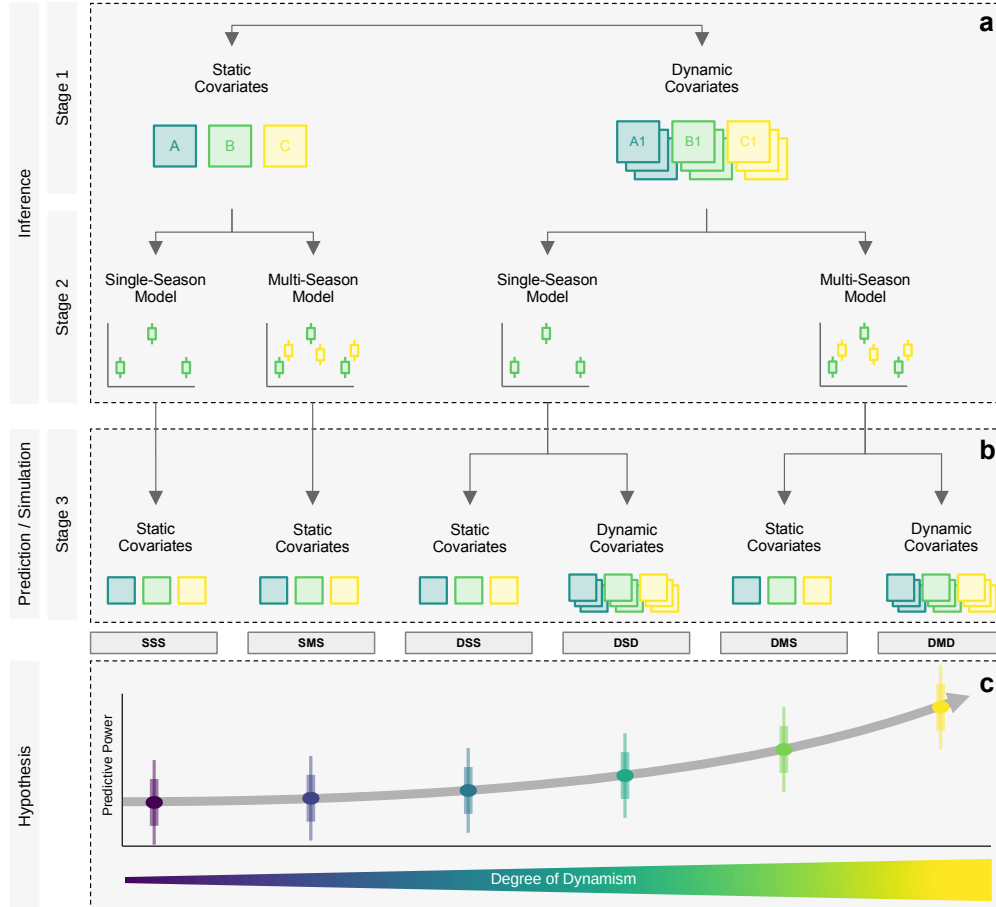


**Figure 1:** Overview of the different dimensions in which seasonality can be rendered in studies of landscape connectivity. (a) During model fitting, the modeler needs to decide whether to represent the environment by a static set of covariate layers, thus ignoring seasonality, or whether to obtain a dynamic set covariate layers that allow rendering it. One also needs to decide whether to parameterize a single-season model, assuming fixed preferences across the year, or to engage in a multi-season model that accounts for seasonal differences. (b) When utilizing the fitted model to predict connectivity, one can either assume a static set of environmental covariates or again attempt a seasonal take that renders how connectivity differs depending on the season. (c) Depending on these decisions, six different combinations with differing degrees of dynamism emerge. Our hypothesis was that increasing the degree of dynamism would lead to improved predictions. However, we were particularly interested in determining at which stage the inclusion of seasonally provided the biggest benefits.

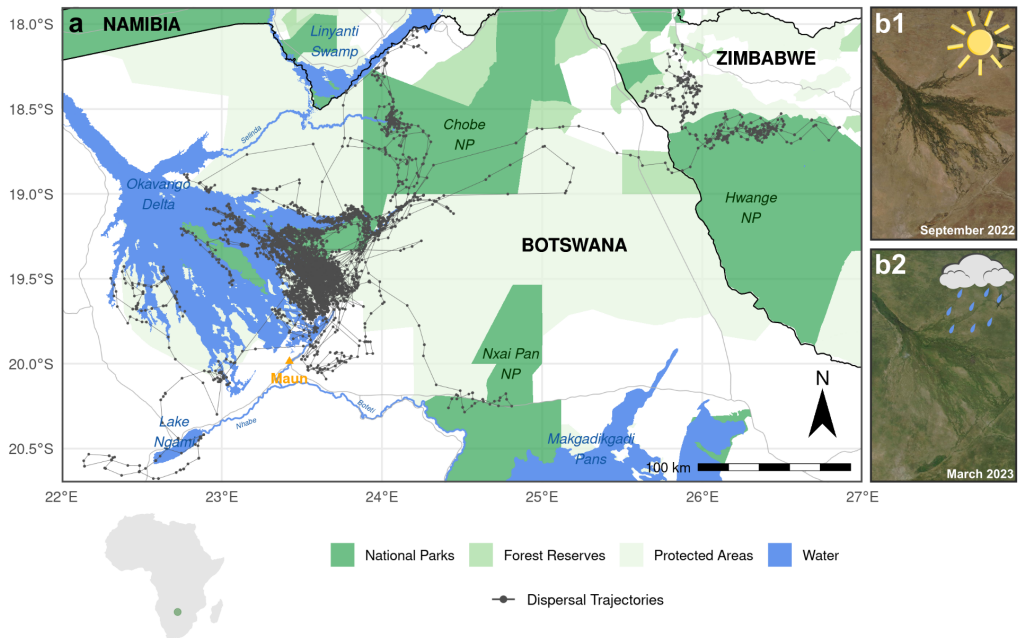


**Figure 2:** (a) Study area from which data on dispersing wild dogs were collected. Dispersal trajectories are plotted in dark gray. The study area encompassed parts of the Okavango Delta in northern Botswana, a highly dynamic, flood-pulse-driven ecosystem. The entire study area undergoes substantial seasonal changes, as can be seen from two satellite images taken during peak dry season (b1) and peak rainy season (b2). Notably, the flood of the Okavango Delta reaches its maximum extent during peak dry season (August–September).

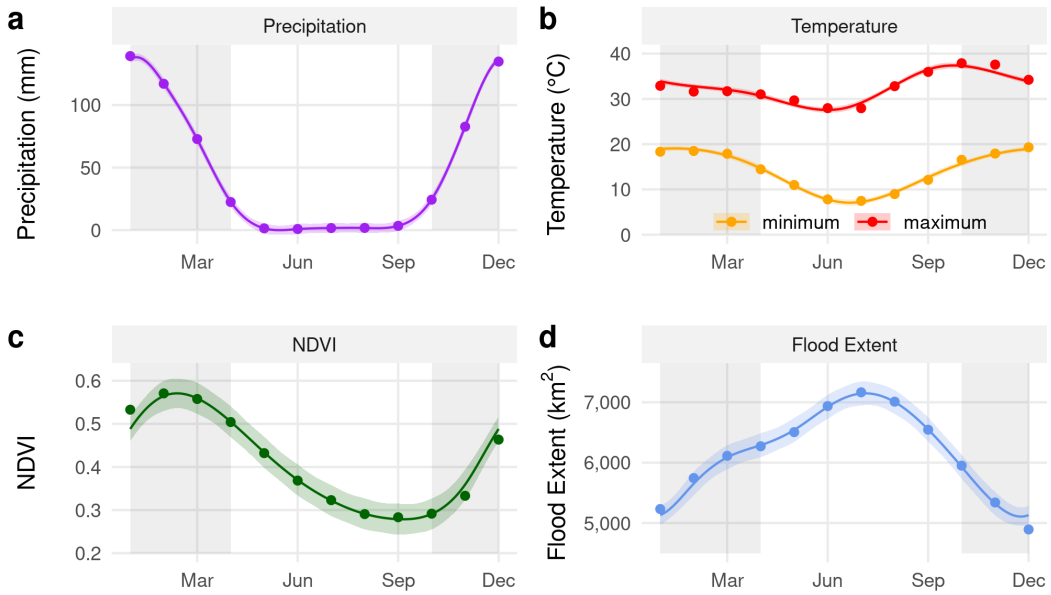


**Figure 3:** Illustration of how some covariates considered in this study vary across seasons. The wet season spans mid-October to mid-April (shaded in gray). Data for the graphs were obtained from (a) JAXA GSMAp, (b) ERA5, (c) MODIS MOD13Q1, and (d) remote sensed MOD43A4 satellite images. Smoothing curves were fitted using GAMs as implemented in the `mgcv` R-package (Wood, 2011).

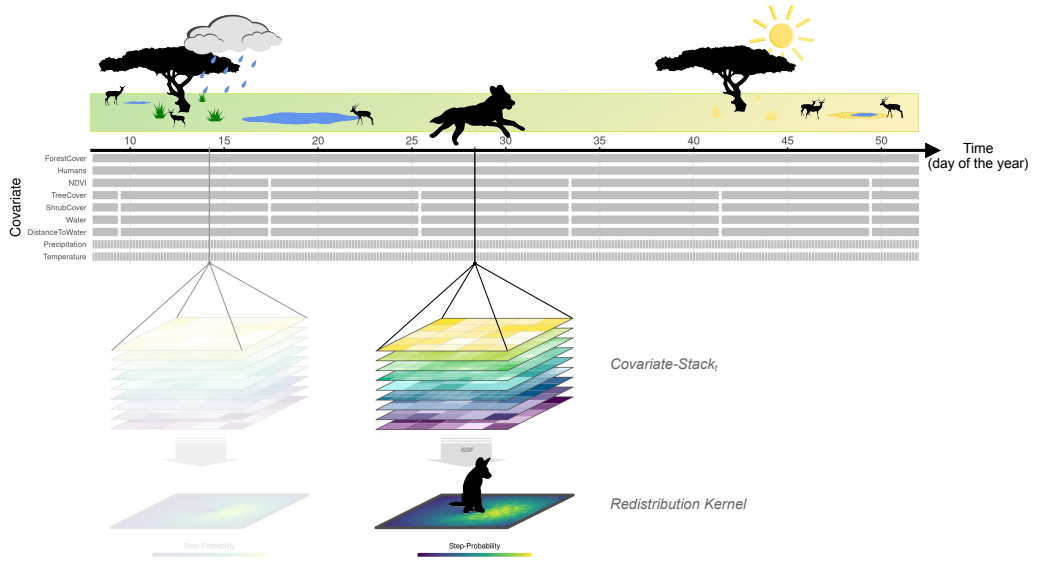


**Figure 4:** Schematic illustration of a dispersal simulation with dynamic covariates. As the simulation proceeds, the underlying covariates (symbolized by the stack of layers) are updated. In our case, the update frequency of covariate layers varied from a few hours (e.g., temperature) to multiple months (e.g., shrub cover). Each gray block represents a single layer and the duration for which it was “active”. Originating from the current position of the simulated animal, a new redistribution kernel is derived. We generated redistribution kernels by proposing a set of random steps and applying the parametrized step-selection model to predict the probability of each step for being chosen. Based on this kernel, one location was randomly sampled and the animal’s position updated. This procedure was repeated until the number of simulated steps matched the number of steps from the observed individuals.

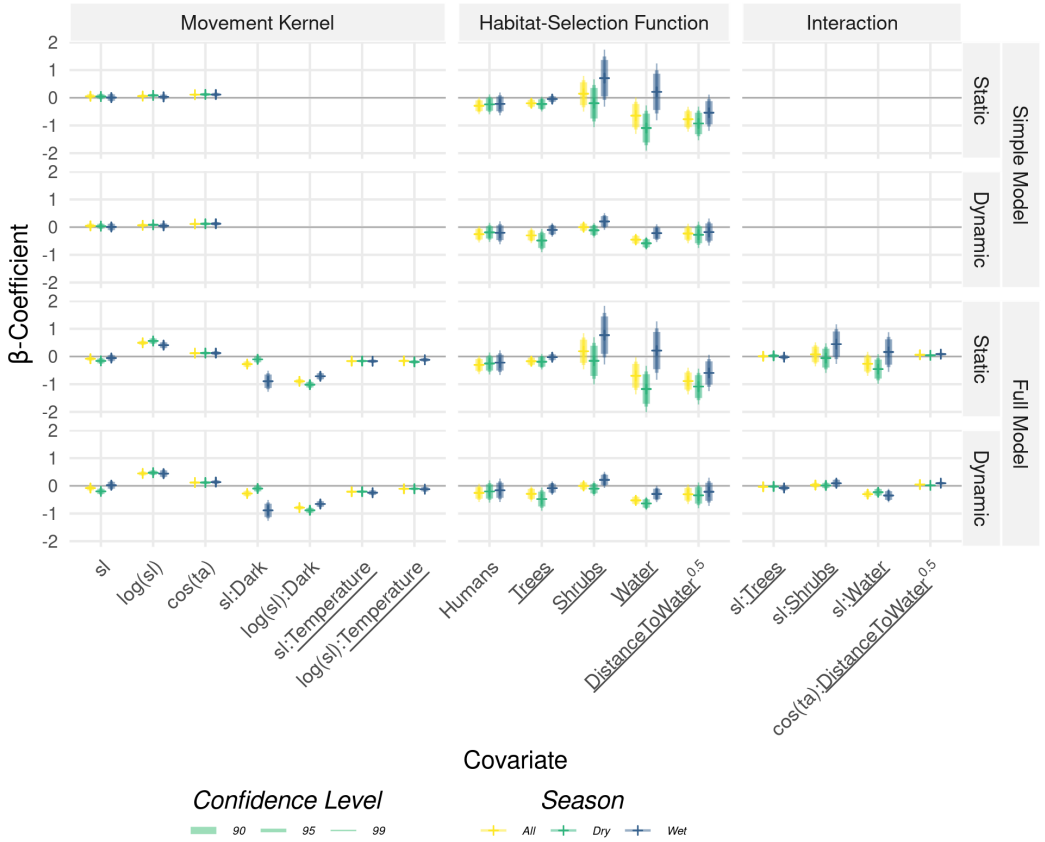


**Figure 5:**  $\beta$ -estimates from the integrated step-selection models, grouped by movement kernel, habitat-selection function, and their interaction. We either fit a simple model without interactions or a full model with interactions and we distinguished between models fit using static or dynamic covariates. Only the underlined covariates differed between the static and dynamic configurations, as covariates were either represented as a single layer (static), or a stack of layers (dynamic). Furthermore, data was either pooled across seasons (yellow bars) or split into dry (green bars) and wet (blue bars) season.

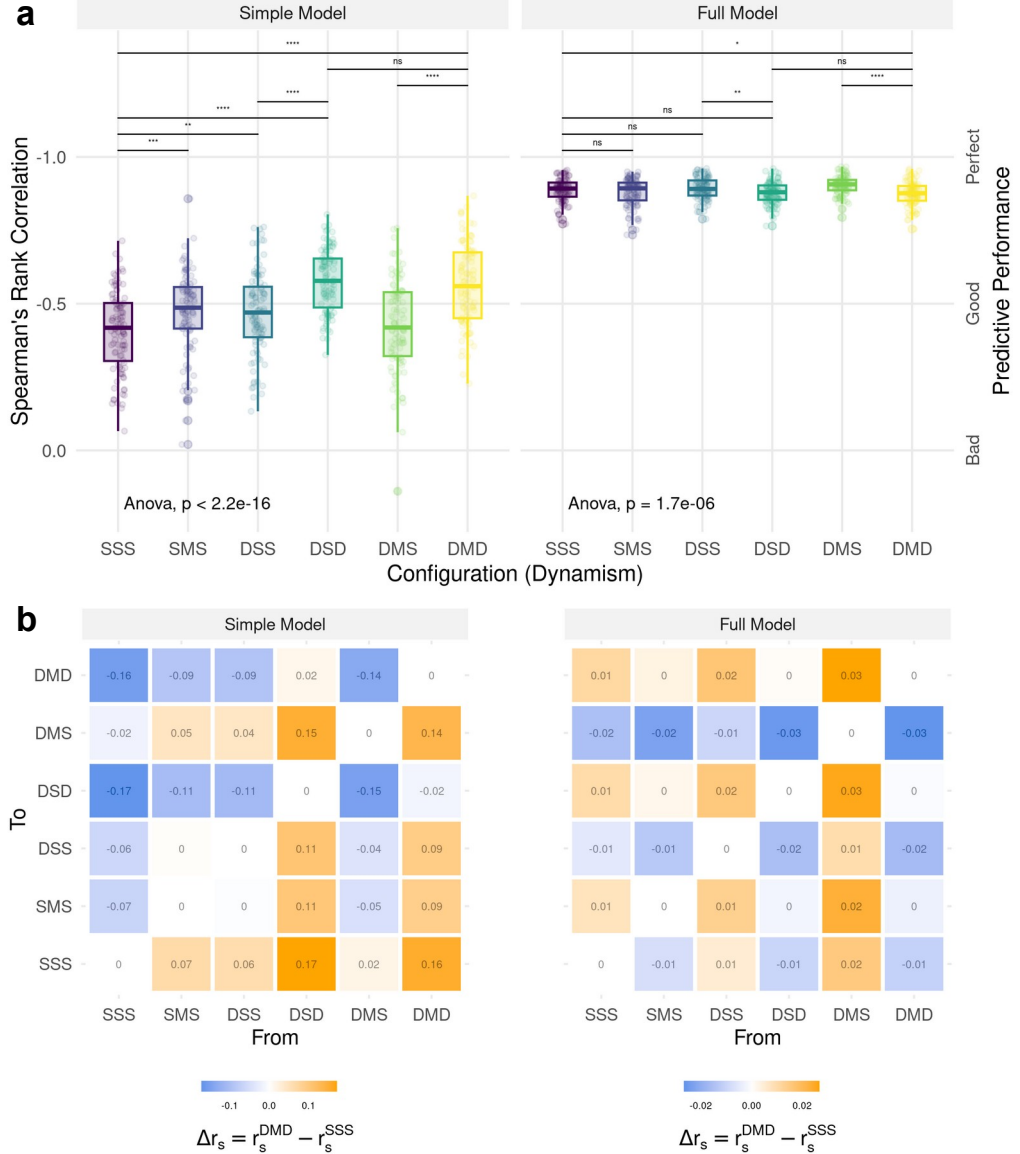


**Figure 6:** (a) Spearman's rank correlation across different configurations of dynamism that range from entirely static (SSS) to fully dynamic (DMD). The more negative Spearman's rank correlation, the better is the predictive performance under the respective configuration. Correlations were computed for 100 replicates. Note that the y-axis is inverted to match our expectation of increasing performance as dynamism increases. (b) Difference in Spearman's rank correlation when moving from one configuration to another. Values  $< 0$  (blue) indicate an increase in predictive performance, whereas values  $> 0$  (orange) indicate a decrease in predictive performance.

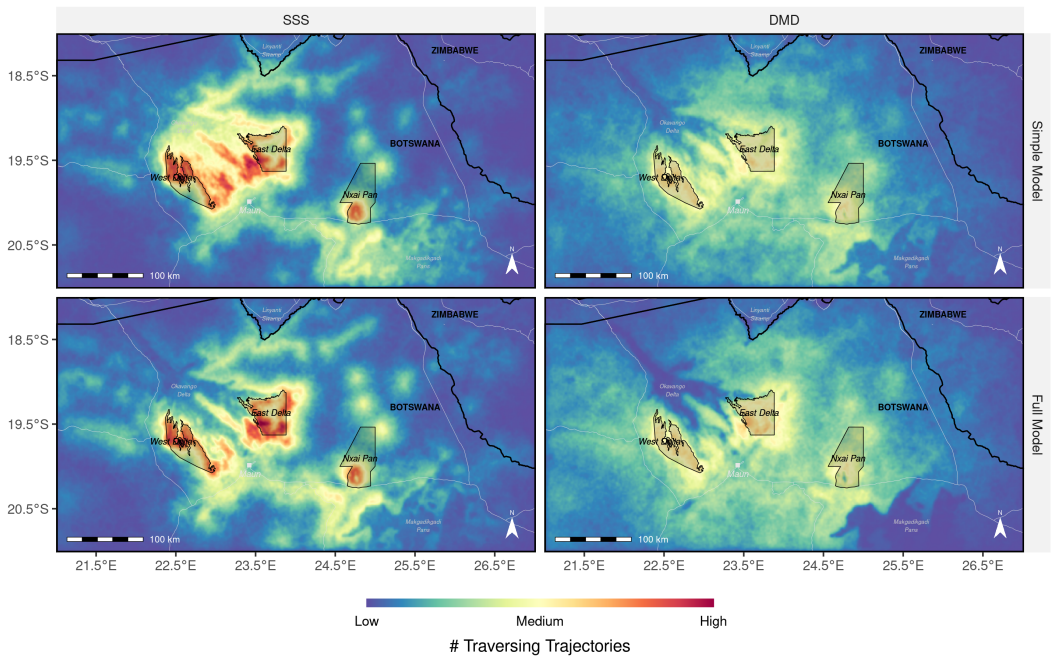


**Figure 7:** Heatmaps derived under the most static (SSS) and dynamic (DMD) configurations. Results are shown for both the simple and full model.

**Table 1:** Covariates that were used in this study, including information on their temporal and spatial resolutions, as well as on the avenue through which the respective data were accessed or downloaded.

Variable	Temporal Resolution	Spatial Resolution	Source	Download Method
(1) Landscape Characteristics				
Trees	1 year	250 m	MODIS MOD44B	RGISTools
Shrubs / grassland	1 year	250 m	MODIS MOD44B	RGISTools
NDVI	16 days	250 m	MODIS MOD13Q1	rgee
Rivers	static	90 m	MERIT Hydro	website
Permanent water	static	30 m	Globeland30	website
Floodwater	8 days	500 m	MOD34A4	floodmapr
Distance to water	8 days	500 m	MOD43A4	floodmapr
Pans	5/10 days	10 m	Sentinel 2	sen2r
Distance to pans	5/10 days	10 m	Sentinel 2	sen2r
(2) Climate Descriptors				
Temperature	4 hours	10 km	ERA5	rgee
Precipitation	4 hours	10 km	JAXA GSMAp	rgee
(3) Anthropogenic Features				
Human density	static	30 m	Facebook	website
Agriculture	static	30 m	Globeland30 / Cropland	website
Roads	static	vectorized	Open Street Map	website
(4) Light Availability				
Night	4 hours	-	-	moonlit
Moon illumination	4 hours	-	-	moonlit

*Note:* The covariates in gray were combined into proxies for water, human influence, and brightness, respectively. The detailed aggregation procedure is described by Hofmann et al. (2021).